

Ordered droplet structures at the liquid crystal surface

I.I. Smalyuh¹, S. Chernyshuk², B.I. Lev^{2,3}, A.B. Nych², U. Ognysta², V.G. Nazarenko²,
and O.D. Lavrentovich¹ (*)

¹*Liquid Crystal Institute and Chemical Physics Interdisciplinary Program, Kent State University,
Kent, OH 44242, USA*

²*Institute of Physics, Prospect Nauki 46, Kyiv-39, 03039, Ukraine*

³*Japan Science and Technology Corporation, Yokoyama Nano-structured
Liquid Crystal Project, Tsukuba Research Consortium, 5-9-9 Tokodai, Ibaraki
300-2635, Japan*

(December 2, 2024)

Abstract

We demonstrate a variety of ordered patterns, including hexagonal structures and chains, formed by colloidal particles (droplets) at the free surface of a nematic liquid crystal (LC). The surface placement introduces a new type of particle interaction as compared to particles entirely in the LC bulk. Namely, director deformations caused by the particle lead to distortions of the interface and thus to capillary attraction. The elastic-capillary coupling is strong enough to remain relevant even at the micron scale when its buoyancy-capillary counterpart becomes irrelevant.

Typeset using REVTeX

*Author for correspondence (e-mail: odl@lci.kent.edu)

2D organization of nanometer- and micrometer-sized colloidal particles at fluid interfaces is a fascinating phenomenon of both fundamental and applied interest. The nature of micron-scale interparticle forces, especially of the attractive nature, remains a subject of an ongoing debate [1–9]. In most cases, the interparticle forces are isotropic and cause hexagonal ordering. Anisotropic interactions can be achieved when the particles are non-spherical [4,5]. Apparently, *the surfaces of anisotropic fluids*, i.e., liquid crystals (LCs), can also support anisotropic interactions and thus a richer variety of ordered patterns as compared to isotropic fluids. Surprisingly, the current knowledge of particle behavior at LC surfaces is rather limited. It is known that small particles might form chains decorating the surface director field [10,11] and that the surface air bubbles can be accompanied by surface point defects [12]. The behavior of particles entirely in the LC bulk is studied much better [13–21]. Because of the anisotropy of molecular interactions at the particle surface (the phenomenon of anchoring [22]), the embedded particle causes elastic director distortions. The most frequently met distortions are of dipole symmetry; they lead to chaining of droplets [13]. Recently, an unexpected and so far unexplained hexagonal structures have been discovered for an array of glycerol droplets assumed to be in the nematic bulk [18–20] and for droplets in smectic membranes [21].

In this work, we use confocal microscopy to demonstrate that placement of colloidal particles (glycerol droplets of radius $R = 1 - 10 \mu\text{m}$) *at the LC surface* leads to attractive interactions and a variety of ordered patterns, including the hexagonal patterns and chains. The attractive interactions can be explained by the elastic-capillary coupling, as the particle-induced director deformations distort the nematic surface.

The glycerol droplets are obtained as in Ref. [18]. A Petri dish containing a layer of glycerol and the nematic LC pentylycyanobiphenyl (5CB, EM Industries) on top of it, is kept at 50°C for 10 min, to facilitate diffusion of the glycerol molecules into the 5CB layer which is in the isotropic phase above $\approx 35^\circ\text{C}$. When the sample is cooled down, solubility of glycerol in 5CB decreases and one observes appearance and growth of glycerol droplets. The droplets might also contain water adsorbed from air [23]. The technique produces droplets of a practically constant radius R in the films of controlled thickness $h = (1 - 100) \mu\text{m}$. The size of droplets is controlled by the cooling rate and thermal cycling. The 5CB film is in the so-called hybrid aligned state, as the director $\hat{\mathbf{n}}$ is parallel to the LC-glycerol interface at the bottom and perpendicular to the air-LC interface at the top.

In order to determine the location of droplets, we use the Fluorescence Confocal Polarizing Microscopy (FCPM) [24]. Two different dyes with well separated absorption and fluorescence bands, fluorescein and Nile red (both purchased from Aldrich), were added in small quantities (0.01 wt %) to tag glycerol and LC, respectively. The Nile red molecules are well oriented by the LC host, which allows one to determine the 3D director patterns [24]. Addition of the dyes did not change the appearance of patterns. The FCPM textures of vertical cross-section of the samples, Fig.1a-c, unambiguously demonstrate that the glycerol droplets are trapped at the LC-air interface. For a better clarity, the images in Fig.1a,b are taken for a relatively large drop; smaller drops are also located at the interface, Fig.1c.

A 4-6 hour relaxation at room temperature results in 2D ordered structures of droplets. The order is of a hexagonal type when the nematic layer is thick, $h \gg R$, $h = (20 - 100) \mu\text{m}$, Fig.2a,b. The time average of the droplet center-to-center separation r increases with the droplets diameter R , Fig.2d; each data point was an average of the data

collected by video-recording the patterns every 6 s for 10 minutes. The angles between the directions to the nearest neighbours changes in the range $60^\circ \pm 8^\circ$ for well-equilibrated structures. At this stage, it is impossible to quantify the lattice symmetry more precisely as it might be influenced by slowly changing director pattern in the bulk.

In thin films, $h/R \approx 2 \div 5$, $h \leq 10\mu m$, Fig.3a, the pattern changes completely, as the droplets form chains oriented along the average horizontal projection of the director field. The length of chains (number of droplets in a chain) increases when h decreases. Importantly, both types of ordered patterns, hexagonal and chain-like, disorganize when the nematic is heated into the isotropic phase.

The very existence of 2D hexagonal-like pattern in thick films does not discriminate between attractive and repulsive interactions among the particles, as in the confined systems such as a Petri dish the ordering can be induced by purely repulsive forces. The presence of repulsive force is manifested clearly, as the droplets are well separated. The following three experiments show that the interaction has also an attractive component. (A) We start with the Petri dish in which the 2D lattice occupies the whole area and then use a filter paper to wipe about 1/2-1/3 of the droplets. The remaining droplets restore the 2D lattice within the smaller area, with the lattice parameter close to the original one. (B) We change the direction of the meniscus tilt near the Petri dish walls by coating the walls with a hydrophobic material (stearin); the types of the 2D ordering remain the same. (C) After the 2D lattice is formed in a regular manner described above, we add (through a microsyringe) a small amount (0.01% by weight) of a surfactant (cetylpyridinium chloride) to the nematic layer. The interparticle distances decrease; the shrank clusters are separated by droplet-free areas, Fig.2c.

What is the mechanism of the droplet attraction? The typical candidates such as gravity-mediated capillary effect and the van der Waals forces appear to be insignificant, as the corresponding pair potentials [25,22]

$$U_g(r) \approx \frac{2\pi R^6}{\sigma_{LCA}} g^2 \rho_{LC}^2 \ln\left(\frac{r}{\lambda}\right); \quad U_{vdW}(r) \approx -\frac{AR}{12(r-2R)}; \quad (1)$$

are of the order of thermal energy $k_B T \approx 4 \times 10^{-21} J$ or less, when r is a few microns. Here $\sigma_{LCA} \approx 3.8 * 10^{-2} J/m^2$ [26] is the LC-air interfacial tension coefficient, $\rho_{LC} \approx 10^3 kg/m^3$ is the LC density, g is acceleration due to the gravity, $\lambda = \sqrt{\sigma_{LCA}/(g\rho_{LC} - \frac{\partial \Pi}{\partial h})}$ is the capillary length; $\Pi \approx K/h^2$ is the elastic disjoining pressure for the hybrid aligned film [22]; $K \sim 10^{-11} N$ is the average nematic elastic constant; in all cases of interest to us, $\lambda \gg r$, as $\lambda \approx 2mm$ when $h \rightarrow \infty$ and $\lambda \approx 0.5mm$ when $h = 5\mu m$; finally, A is the Hamaker constant of the order of $10^{-19} J$ or smaller [22].

Attraction of droplets at the nematic surface (and absence of attraction and regular patterns when the LC is heated into the isotropic phase) can be explained by the coupling of orientational elasticity and capillarity. As demonstrated by de Gennes [27], director distortions in the bulk are capable of changing the profile of the nematic-air interface. The distortions, caused in our case by the submerged part of the particle, give rise to a vertically resolved force f_{el} that shifts the LC-air interface upward or downward, depending on the particle properties, to reduce the elastic energy of the host. Non-flat interface causes long-range attraction of particles. As the first approximation, we divide the total potential $U(r)$

of interaction into two parts, $U_{elc}(r)$ describing the elastic-capillary coupling and $U_{elb}(r)$ for the "pure bulk" elastic coupling.

To estimate the orders of magnitude, we use the idea that f_{el} is related to the non-vanishing surface anchoring of $\hat{\mathbf{n}}(r)$ at the LC-particle interface:

$$f_{el} = \frac{\partial}{\partial z} E_{el}(z) \sim \frac{\partial}{\partial z} \oint_{\Omega(z)} W(\hat{\mathbf{n}} \cdot \hat{\nu})^2 ds, \quad (2)$$

where $E_{el}(z)$ is the total elastic energy of distortions caused by the particle, $\Omega(z)$ is part of the droplet surface immersed in the LC, W is the (polar) anchoring coefficient of the LC-glycerol interface, $\hat{\nu}$ is the normal to the interface, and z is the vertical coordinate of some fixed point, say, the bottom of the droplet. For $f_{el} \approx 4\pi WR$, with $W = 10^{-5} J/m^2$ [22], one finds $f_{el} \sim 10^{-10} N \sim 10K$ when $R = 1\mu m$. The force f_{el} replaces the buoyancy force in the standard treatment [3,25]; it is balanced by the surface tension, hence, $f_{el} = 2\pi\sigma_{LCA}r_i \sin\psi$, where ψ is the meniscus slope at the triple contact line of radius r_i . The vertical displacement $\xi(r) \approx -r_i \sin\psi \ln \frac{r}{\lambda}$ changes the interfacial area and leads to the attractive potential written for two identical particles as $U_{elc} = -f_{el}\xi$, or

$$U_{elc}(r) = \frac{f_{el}^2}{2\pi\sigma_{LCA}} \ln\left(\frac{r}{\lambda}\right), \quad (3)$$

first derived for the buoyancy case [3,25]. For $f_{el} \sim 10K$, one estimates $U_{elc} \sim 3 \times 10^{-19} J \sim 80 k_B T$. Therefore, the coupling between the orientational elasticity and capillarity is strong enough to cause attraction between the droplets. Importantly, the dependence $U_{elc}(R)$ is weaker than $U_g(R) \propto R^6$ of the gravity mechanism, as $E_{el}(R) \sim WR^2$ for $R \ll K/W$, and $E_{el}(R) \sim KR$ for $R \gg K/W$ [22]. The elastic-capillary effect remains strong at micron scales where the gravity effect vanishes.

We turn now to the estimates of the "pure bulk" interactions. In the hybrid aligned film, the director pattern is determined by the balance of anchoring and elasticity. For $h \gg K/W$, $\hat{\mathbf{n}}$ at the LC-air interface is vertical; as h decreases, $\hat{\mathbf{n}}$ deviates from the vertical axis and becomes progressively horizontal (the anchoring coefficient at the air interface is smaller than W [28]). Tangential anchoring of $\hat{\mathbf{n}}$ at the droplet surface leads to a point defect-boojum [22], Fig.1e.

In the thick films, the boojum is close to the south pole, Fig.2e, and the director distortions around the droplets can be approximated by an elastic dipole normal to the LC-air interface [13], $\mathbf{p} \approx (0, 0, \alpha_z R^2)$, where α_z is a numerical constant. The bulk interaction in this case is nearly isotropic (in the plane of the film) and repulsive,

$$U_{elb,thick}(r) = K \frac{\alpha_z^2 R^4}{r^3}. \quad (4)$$

Here and in what follows we neglect the fast-decaying quadrupole effects [13,14]. The pair interaction potential, $U_{total} = U_{elc} + U_{elb,thick}$, has a clear minimum at

$$r_{eq}^{pair} = \left(\frac{6\pi\alpha_z^2\sigma_{LCA}R^4K}{f_{el}^2} \right)^{1/3}. \quad (5)$$

For example, $r_{eq}^{pair} = 13\mu m$ for $f_{el} = 10^{-10} N$, $\alpha_z = 0.2$ and $R = 3\mu m$. Interestingly, for $f_{el} \propto WR$, Eq.(5) predicts $r_{eq}^{pair} \propto R^{2/3}$, namely, $r_{eq}^{pair} = \gamma(\sigma_{LCA}R^2K/W^2)^{1/3}$, where γ is a

dimensionless constant. The trend is in agreement with the experimental data in Fig.2d, despite the fact that Eq.(5) is derived from the pair potential. Note that the dependence $f_{el}(R)$ might be different from linear, depending on the elastic and anchoring parameters (such as anchoring at the nematic-air interface, director distortions in the meniscus region, etc.). In addition, f_{el} might be r -dependent, in which case the form of $U_{total}(r)$ with one minimum at r_{eq}^{pair} and attractions for any $r > r_{eq}^{pair}$ will modify. For example, our experiments show that when the concentration of droplets is low and the initial separation is large, $r > (5 - 10)R$, the ordered structures do not form. Note also that addition of surfactant changes σ_{LCA} and f_{el} and thus offers a simple method to control the patterns, as observed in the experiments.

In the thin nematic films, the boojum shifts to the side of the droplet, Fig.3b, giving rise to the in-plane elastic dipole component, $p_x = \alpha_x R^2$, and the anisotropic contribution to the potential of interaction

$$U_{elb,thin}(r, \theta) = K \frac{\alpha_x^2 R^4}{r^3} (1 - 3 \cos^2 \theta), \quad (6)$$

that depends on the angle θ between the radius-vector connecting the two droplets and the direction of their dipole moments. The tendency of droplets to form chains at the surface of thin nematic films can thus be explained similarly to the chaining observed for droplet-hedgehog pairs entirely in the nematic bulk, i.e., through the angular dependence of $U_{elb,thin}$ [13]: the minimum of $U_{elb,thin}$ is achieved when the in-plane components of the dipole moments are parallel to the separation direction, $\theta = 0$; quadrupolar interactions might change this value.

To conclude, the particles (glycerol droplets) at the LC-air interface are capable of both repulsive and attractive interactions that lead to ordered patterns of hexagonal and chain types. The director distortions in LC give rise to a vertical elastic force balanced by surface tension; the deviation of the LC-air interface from the horizontal plane results in attraction of droplets. The phenomenon appears to be general, as we observe hexagonal patterns not only for the liquid droplets but also for micron-size polymer balls at the nematic-air interface; these results will be published elsewhere. The observed interplay of bulk and surface properties of LCs can be used in a controlled assembly of micro- and nanoparticles and in LC sensors [29].

We acknowledge helpful discussion with M. Kleman, V. Pergamenschik, S.V. Shiyonovskii, P. Tomchuk, and H. Yokoyama. The work was supported by National Science Foundation Grant DMR-0315523 and STCU grant #2025.

Figure captions.

FIG.1. Two-channel FCPM textures of the vertical cross-section of the LC film: (a,b) a single glycerol droplet at the LC-air interface; (c) a row of droplets that is a part of a hexagonal pattern at the LC-air interface; (d) scheme of forces and interfacial tension vectors at the LC-air interface with a strongly exaggerated meniscus slope; (e) 3D director field in the LC layer. The LC layer (glycerol droplet) is manifested by the high (low) intensity of fluorescent light in parts (a,c); the contrast is opposite in (b).

FIG.2. Optical microscopy pictures of hexagonal structures at the free surface of the thick nematic layer, $h \approx 60\mu m$, formed by droplets of different average diameter: (a) $2R \approx 7\mu m$, (b) $2R \approx 1\mu m$. (c); arrangement of droplets after the surfactant is added to the nematic layer; (d) droplets separation r vs. $2R$; the data are compared to the dependence $r_{eq}^{pair} = \gamma(\sigma_{LCA}R^2K/W^2)^{1/3}$, where $\gamma = 0.43$, $K = 10^{-11}N$, $\sigma_{LCA} = 3.8 \times 10^{-2}J/m^2$, $W = 10^{-5}J/m^2$, see the text; (e) schematic drawing of the director field in the top part of the LC layer.

FIG.3. Optical microscopy textures of glycerol droplets forming chains at the free surface of a thin LC layer, $h \approx (7 - 10)\mu m$ (a) and the corresponding director field scheme (b).

REFERENCES

- [1] P. Pieranski, *Contemp. Phys.* **24**, 25 (1983).
- [2] R.E. Kusner, J.A. Mann, J. Kerins, and A.J. Dahm, *Phys. Rev. Lett.* **73**, 3113 (1994).
- [3] P. A. Kralchevsky and K. Nagayama, *Advances in Colloidal and Interface Science*, **85**, 145 (2000)
- [4] A.B.D. Brown, C.G. Smith, and A.R. Rennie, *Phys. Rev. E* **62**, 951 (2000)
- [5] D. Stamou, C. Duschl, D. Johannsmann, *Phys. Rev. E* **62**, 5263 (2000)
- [6] K. Zahn, A. Wille, G. Maret, S. Sengupta, and P. Nielaba, *Phys. Rev. Lett.* **90**, 155506 (2003)
- [7] M.G. Nikolaides, A.R. Bausch, M.F. Hsu, A.D. Dinsmore, M.P. Brenner, C. Gay, and D.A. Weitz, *Nature* **420**, 299-301 (2002) and **424**, 1014 (2003).
- [8] M. Megens and J. Aizenberg, *Nature* **424**, 1014 (2003).
- [9] Y. Han and D.G. Grier, *Phys. Rev. Lett.* **91**, 038302 (2003).
- [10] J. Rault, *C.R. Acad. Sci. Ser.B* **272**, 1275 (1971).
- [11] P. Cladis, M. Kleman, and P. Pieranski, *C.R. Acad. Sci. Ser.B* **273**, 275 (1971).
- [12] R.B. Meyer, *Mol. Cryst. Liq. Cryst.* **16**, 355 (1972).
- [13] P. Poulin, H. Stark, T.C. Lubensky, and D.A. Weitz, *Science* **275**, 1770 (1997).
- [14] B. I. Lev and P. M. Tomchuk, *Phys. Rev. E* **59**, 591 (1999).
- [15] A. Borstnik, H. Stark and S. Žumer, *Phys. Rev. E* **60**, 4210 (1999).
- [16] J.-Ch. Loudet, P. Barois, and P. Poulin, *Nature* **407**, 611 (2000).
- [17] S. P. Meeker, W. C. K. Poon, J. Crain, and E. M. Terentjev, *Phys. Rev. E* **61**, R6083 (2000).
- [18] V. G. Nazarenko, A. B. Nych, and B. I. Lev, *Phys. Rev. Lett.* **87**, 075504 (2001).
- [19] B. Lev, A. Nych, U. Ognysta, D. Reznikov, S. Chernyshuk, and V. Nazarenko, *Pis'ma Zh. Exp. Teor. Fiz.* **75**, 393 (2002) [*Sov. Phys. JETP Lett.* **75**, 322 (2002)].
- [20] T. Yamamoto, J. Yamamoto, B.I. Lev, and H. Yokoyama, *Appl. Phys. Lett.* **81**, 2187 (2002).
- [21] P. V. Dolganov, E.I. Demikhov, V.K. Dolganov, B.M. Bolotin, and K. Krohn, *Eur. Phys. J. E* **12**, 593 (2003).
- [22] M. Kleman and O.D. Lavrentovich, *Soft Matter Physics: An Introduction* (Springer-Verlag, New York, 2003).
- [23] P. Pieranski, private communication.
- [24] I.I. Smalyukh, S.V. Shiyankovskii, and O.D. Lavrentovich, *Chem. Phys. Lett.* **336**, 88 (2001).
- [25] D. Y. C. Chan, J. D. Henry, and L. R. White, *J. Colloid Interface Sci.* **79**, 410 (1981).
- [26] M. Tintaru, R. Moldovan, T. Beica, and S. Frunza, *Liq. Cryst.* **28**, 793 (2001).
- [27] P.G. de Gennes, *Solid State Comm.* **8**, 213 (1970).
- [28] O.D. Lavrentovich and V.M. Pergamenschik, *Phys. Rev. Lett.* **73**, 979 (1994).
- [29] J.M. Brake, M.K. Daschner, Y.Y. Luk, N.L. Abbott, *Science* **302**, 2094 (2003).

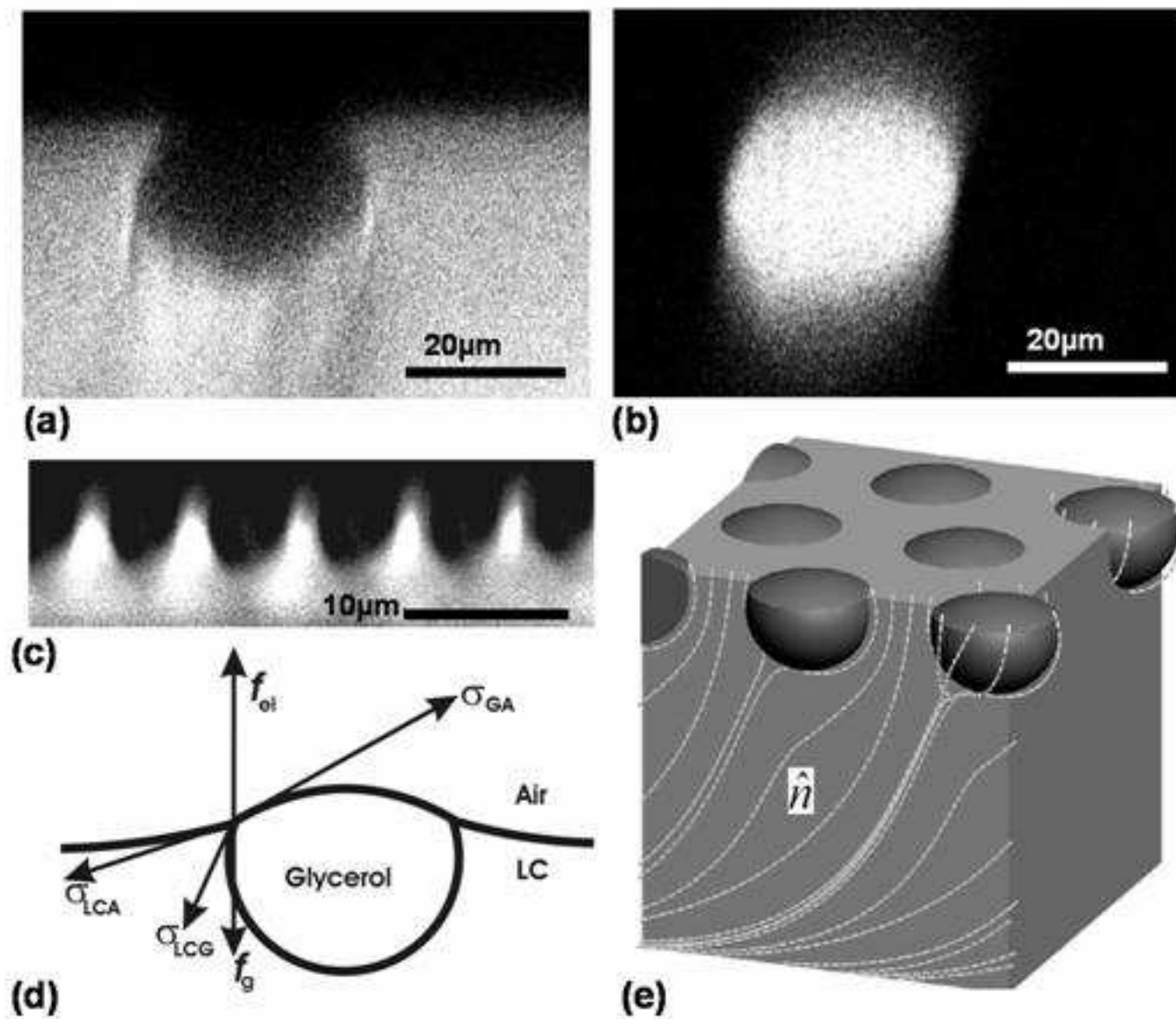


FIG.1

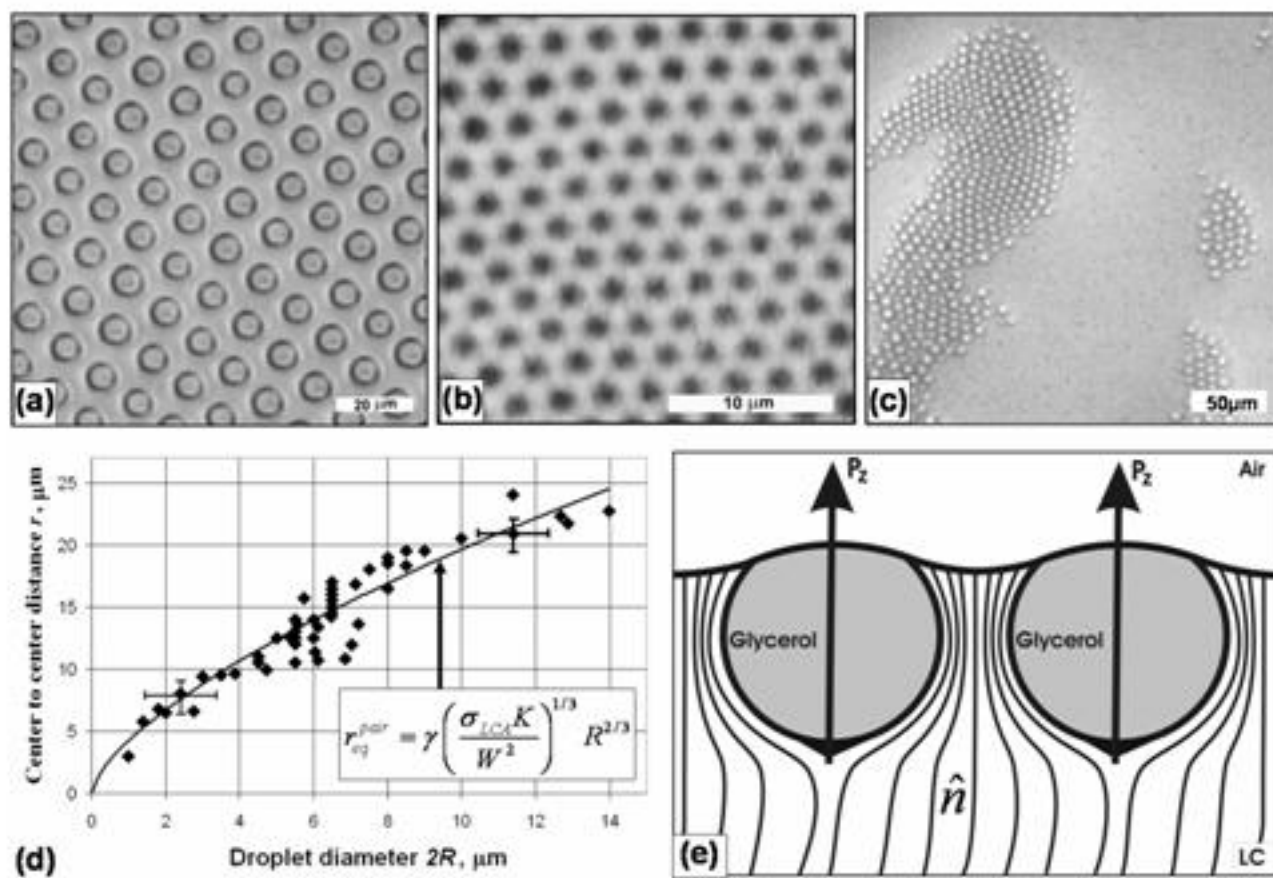


FIG.2

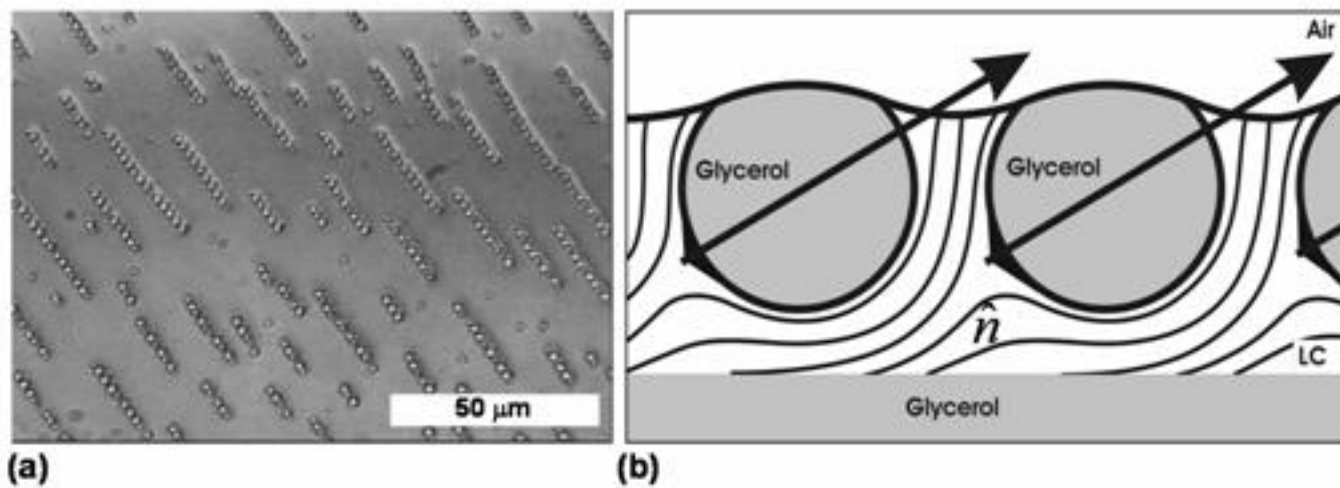


FIG.3